An Improved Gamma Scanning Assay Method for the 400-L Compacted Radioactive Waste Drum Based on the Segmented Equivalent Ring Source

Weiguo Gu, Dezhong Wang, Xinhai Tang, and Yuanwei Ma

***Abstract*— An improved characterization assay algorithm for the 400-L low- and intermediate-level radioactive waste drum was developed based on the segmented equivalent ring source. The improved method (IM) was validated by experiments on a 200-L waste drum. The assay errors are smaller than that of segmented gamma scanning (SGS). Numerical measurements were performed on a 400-L waste drum with two densities of 1.5 and 2.5 g/cc. Three common nuclides, Ba-133, Cs-137, and Co-60, were selected. The results show that the source positions can be determined using two detectors through this method. The maximum error of the IM is several times smaller than that of SGS if the matrix is uniformly distributed in the waste drum. The mean errors are reduced by one third to half for all nuclides compared with SGS. If IM is applied in assaying the solidified wastes drum that contains one or two cylindrical iron products, the strong attenuation of gamma rays by irons and concretes will affect the determination of source positions. The assay accuracy decreases in this case, but it is overall better than that of SGS. The results indicate that IM is an accurate method for assaying the compacted waste drums with nonuniformly distributed radioactive sources.**

***Index Terms*— 400-L compacted radioactive waste, equivalent ring source, improved gamma scanning method, nondestructive assay.**

I. Introduction

RADIOACTIVE wastes must meet the acceptance criteria required by the national regulatory and management authorities. It is necessary to assay the activities and categories of radioactive nuclides inside waste drums before the final disposal.

The segmented gamma scanning (SGS) technique [1] is one of the most widely used nondestructive methods to determine the nuclide activity. Gamma rays emitted from the radioactive waste are attenuated by the large volume waste. The SGS assumes that both matrix and radionuclides are homogeneously distributed. The large assay errors therefore appear when the distribution is not homogeneous [2]. To solve this problem, the tomographic gamma scanning (TGS) method was proposed by dividing a drum into small voxels and reconstructing matrix density and activities of nuclides in these voxels [3]. The assay process of TGS is more complex and time-consuming than the SGS. In order to improve the detection accuracy, some new and improved gamma-ray scanning approaches, including the dynamic grids [4], [5] and semi-TGS [6] techniques were proposed mainly aiming at the 200-L waste drum to reduce the number of voxels. In order to reduce the amount of waste drums, the wastes are compacted in the 400-L drum. The increase of volume and density will result in more attenuation of gamma rays and larger assay errors.

The assay error of SGS is mainly associated with the unknown spatial distribution of radioactive sources in the compacted wastes [7]. An improved SGS method was studied for 200-L drums where point sources are approximated to ring sources when a waste drum is rotated continuously [8]. Under this assumption, the weighted average radii of ring sources are calculated. The relationship between gamma-ray counts and activity can be established according to the equivalent source position. The activity of a nuclide obtained by this method is more accurate than that by SGS. However, the algorithm is incomplete. Large errors would appear when the source number and matrix density increase. Another method to locate the source position is to combine gamma emission tomography with SGS [9]. The SGS is applied first to scan the drum by moving the detector along the drum axis to find segments containing point sources. The emission tomography is then used to reconstruct an activity image in active segments. However, this method is difficult to distinguish a point source from homogeneously distributed sources. If the distribution is homogeneous, gamma emission tomography is not necessary.

Therefore, aiming at the 400-L low- and intermediate-level radioactive waste drum with high density, this paper proposes an improved gamma scanning method to assay the nuclide activity quantitatively based on the assumption that each radioactive source is equivalent to one segmented ring source. This method is feasible for the large-volume, compacted waste drum when the matrix is assumed to be distributed homogeneously.

Manuscript received March 24, 2019; accepted May 19, 2019. Date of publication May 31, 2019; date of current version July 16, 2019. This work was supported in part by the National Natural Science Foundation of China under Grant 11575113 and in part by the Key Program of the National Natural Science Foundation of China under Grant 11535009.

The authors are with the School of Mechanical Engineering, Shanghai Jiao Tong University, Shanghai 200240, China (e-mail: dzwang@sjtu.edu.cn).

Color versions of one or more of the figures in this paper are available online at http://ieeexplore.ieee.org.

Digital Object Identifier 10.1109/TNS.2019.2920180

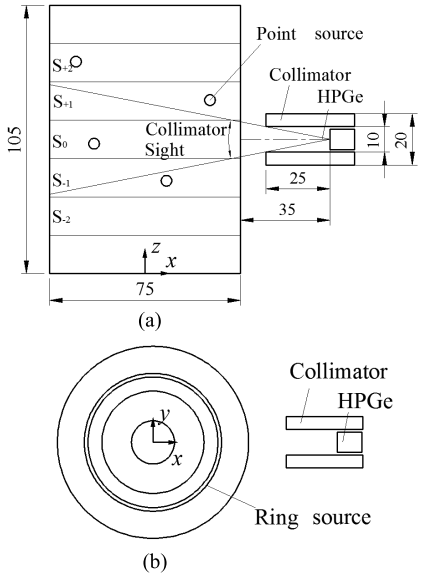

Fig. 1. Schematic layout of the gamma scanning method. (a) Layout in x-z plane. (b) Layout in x-y plane.

II. Principles

As shown in Fig. 1, the high-purity germanium (HPGe) detector with a lead collimator is employed in the detection system. The waste drum is divided into several vertical segments. The detector will be lifted step by step to scan the waste drum and count the gamma rays. When the detector is at a vertical position, the gamma rays received by the detector are contributed by all emission sources. If the matrix is homogeneous in the waste drum, the point sources can be regarded as concentric ring sources with the same activity when the drum rotates several circles at a constant speed. In this situation, the count rate (C_k) of a characteristic gamma ray emitted by one nuclide is defined by the following equation:

$$C_k = \alpha \sum_{n=1}^{N} A_n E_{nk} \tag{1}$$

where k represents the position number of the detector If the point sources contain the same nuclide, they are numbered from 1 to N in the waste drum. In (1), α is the branching ratio of the gamma line, A_n is the activity of the nth point source, E_{nk} is the detection efficiency of the equivalent ring source relative to the detector at the kth vertical position. The detection efficiency (E_{nk}) depends on the matrix density, the radius of the ring source, and the detector position relative to the source.

The detection efficiency of the ring source is shown in Fig. 2. In this figure, the abscissa represents the polar radius of the ring source centerline, the ordinate represents the detection efficiency of Cs-137 when the matrix density is 2.5 g/cc. The 400-L waste drum is divided into seven segments. The label "Segment ±0" denotes the ring sources in the segment with the same height to the detector; "Segment ±1" and "Segment ±2" denote the ring sources located in the segments above or below the detector by one and two times of

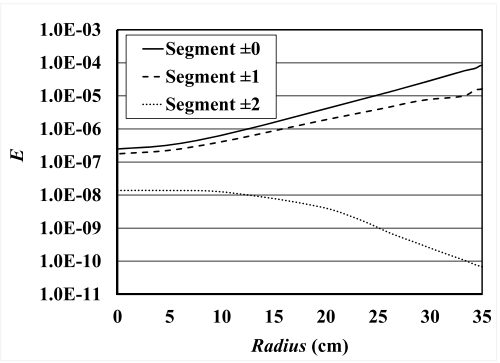

Fig. 2. Detection efficiency of the ring source containing the nuclide Cs-137 against the ring radius when the matrix density is 2.5 g/cc.

segment height. Due to the limited vision of the collimator shown in Fig. 1, the detection efficiency of the ring source labeled "Segment ±2" in Fig. 2 is less than that labeled "Segment ±0" and "Segment ±1S" by more than 1 order of magnitude. Accordingly, (1) can be simplified to

$$C_k = \alpha \left(\sum_{n \in S_{K-1}} A_n E_n^{-1} + \sum_{n \in S_K} A_n E_n^{0} + \sum_{n \in S_{K+1}} A_n E_n^{+1} \right) \tag{2}$$

where the count rate (C_k) of a given nuclide in the kth vertical position consists of three parts contributed by the segments labeled as S_{k-1}, S_k, and S_{k+1} which are below, level with, and above the kth segment, respectively. E_n^{-1}, E_n^0, and E_n^{+1} are the detection efficiencies of the nth ring source located in the segment labeled by S_{k-1}, S_k, or S_{k+1}. Because each source will be scanned successively by the detector from the position below the source to the position above the source by one segment height, E_n^{-1} and E_n^{+1} are similar for one identical source, so they can be represented together by E_n^+. The sum of count rates by the detector at all vertical positions can be expressed by follows:

$$\begin{aligned} C &= \sum_{k=1}^{K} C_k \\ &= \alpha \sum_{k=1}^{K} \left(\sum_{n \in S_k} A_n E_n^0 + \sum_{n \in S_{k-1}} A_n E_n^+ + \sum_{n \in S_{k+1}} A_n E_n^+ \right) \\ &= \alpha \sum_{n=1}^{N} A_n \left(E_n^0 + 2E_n^+ \right) - \alpha \sum_{n \in S_1} A_n E_n^+ - \alpha \sum_{n \in S_K} A_n E_n^+. \end{aligned} \tag{3}$$

Equation (3) shows that the detection efficiency is the sum of E_n^0 and twice E_n^+, but not with E_n^+ when the detector is located below the first segment and above the Kth segment because the assay is absent in the two locations. This is called "end loss." To solve this problem, one method is to complete the assay process. The detector starts from the position below S_1 and ends at S_{K+1}. The other method is to estimate the activities of nuclides in the first and Kth segments according

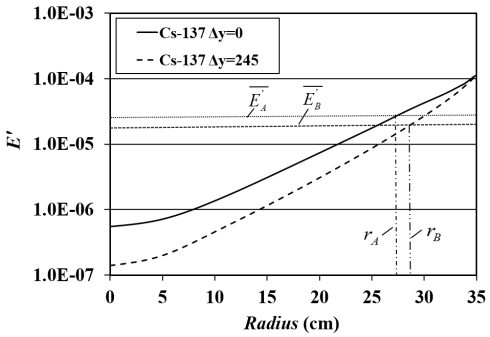

(a)

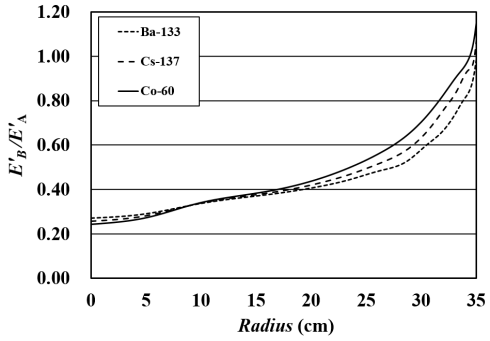

(b)

Fig. 3. Curves of synthetic detection efficiencies and relative detection efficiencies against the source radius when the matrix density is 2.5 g/cc. (a) The synthetic detection efficiencies. (b) The relative synthetic detection efficiency for the detector at position A to that at position B.

to the mean activity in the whole waste drum. If the second method is adopted, (3) can be changed to

$$C = \alpha \sum_{n=1}^{N} A_n \left(E_n^0 + 2\frac{K-1}{K} E_n^+ \right). \tag{4}$$

The synthetic detection efficiency E_n' is defined as

$$E_n^{'} = \alpha \left(E_n^0 + 2\frac{K-1}{K} E_n^+ \right).$$

The total count rate can be expressed by follows:

$$C = \sum_{n=1}^{N} A_n E_n'. \tag{5}$$

In this situation, the synthetic detection efficiency (E_n') is dependent on the radius of the ring source, nuclide type, and matrix density, but independent on source vertical position. All sources in the waste drum can be, therefore, treated to be in one segment. Because the synthetic detection efficiency (E_n') is the weighted sum of E^0 and E^+ which increase monotonically with ring source radius as shown in Fig. 3 (a), all concentric ring sources can be approximated as one ring source with a particular radius of r. This ring source is called as the segmented equivalent ring source, and r is the equivalent radius. Then (5) can be changed to

$$C = E_r^{'} \sum_{n=1}^{N} A_n \tag{6}$$

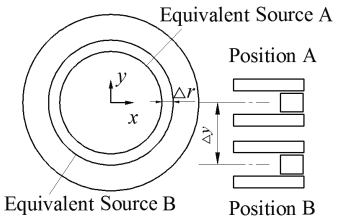

Fig. 4. Schematic of assaying the equivalent ring source based on two detectors.

where E_r' is the synthetic detection efficiency of the segmented ring source with an equivalent radius of r. So far, the total activity (A) of a given nuclide in the waste drum can be derived if the equivalent radius (r) is determined

$$A = \sum_{n=1}^{N} A_n = \frac{C}{E_r'}. \tag{7}$$

Two detectors as shown in Fig. 4 are applied to determine the equivalent radius. The detectors are set at positions A and B. Position A is aligned to the drum center and position B deviates from the center line with an offset of y. The total count rates in positions A and B are respectively given as

$$\begin{cases} C_{\mathrm{A}} = E'_{A,r} \sum_{n=1}^{N} A_n \\ C_{\mathrm{B}} = E'_{B,r+\Delta r} \sum_{n=1}^{N} A_n \end{cases} \tag{8}$$

where E'_{A} and E'_{B} are the synthetic detection efficiencies when the detector is located at positions A and B, respectively. Fig. 3(a) shows the curves of E'_{A} and E'_{B} of the ring source containing Cs-137 located in different radial positions in the waste drum. The matrix is a type of concrete with a density of 2.5 g/cc. The offset (Δy) is 24.5 cm. It can be seen that the two curves have different growth rate against the source radius. Then, the equivalent radius will be different for the detector located at positions A and B. For the uniform distribution of nuclides, the synthetic detection efficiencies $\overline{E'_{\mathrm{A}}}$ and $\overline{E'_{\mathrm{B}}}$ are the mean values of the curves shown in Fig. 3(a), and the equivalent radii are r_{A} and r_{B} accordingly. $\Delta r = r_{\mathrm{B}} - r_{\mathrm{A}}$ is the bias between r_{A} and r_{B}. Certainly, if there is only one source in the segment, Δr is zero.

Aiming at the 400-L waste drum with the matrix whose density is 1.5 or 2.5 g/cc, Δr has been obtained by statistical analysis on 200 drums, where several radioactive sources are randomly distributed. The mean value of Δr is shown in Table I. It is found that Δr ranges from 0.4 to 2.2 cm, depending on the types of nuclides, number of sources, and waste density. However, when the number of sources is beyond 21, Δr will not grow anymore. Because it is difficult to estimate the source number in the waste drum, the mean value is adopted.

In (8), if the count rate C_{B} is divided by C_{A}, the count rate ratio ($C_{\mathrm{B/A}}$) only depends on the ratio of two synthetic

TABLE I

EQUIVALENT RADIUS BIAS (Δr, cm) BETWEEN POSITIONS A AND B FOR 400-L WASTE DRUM

Density		1.5 g/cc			2.5 g/cc		
Nuclide		Ba-133	Cs-137	Co-60	Ba-133	Cs-137	Co-60
Sources number	2	0.5	0.7	0.9	0.3	0.4	0.6
	7	1.3	1.6	2.0	0.7	1.1	1.4
	14	1.4	1.7	2.1	0.9	1.2	1.5
	21	1.4	1.7	2.2	0.9	1.2	1.5

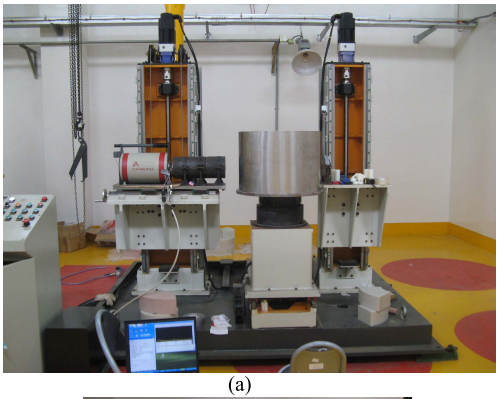

(a)

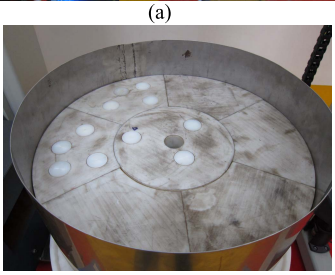

(b)

Fig. 5. Photograph of experimental facilities. (a) Gamma scanning detection system. (b) Polyamide matrix with density of 1.15 g/cc.

detection efficiencies

$$C_{\mathrm{B/A}} = \frac{C_{\mathrm{B}}}{C_{\mathrm{A}}} = \frac{E'_{B,r+\Delta r}}{E'_{A,r}}. \tag{9}$$

A function (F) is defined as follows:

$$F(r) = \frac{E'_{B,r+\Delta r}}{E'_{A,r}}. \tag{10}$$

The curves of F against the ring source radius for nuclides Ba-133, Cs-137, and Co-60 are shown in Fig. 3 (b). The figure shows that the function F monotonically increases when source radius becomes larger, so the equivalent radius (r) can be determined uniquely according to the count rate ratio ($C_{\mathrm{B/A}}$) by (9). So far, accurate detection efficiency can be calibrated if the equivalent radius is deduced. Finally, the total activity can be obtained by (7).

III. RESULTS AND DISCUSSION

The experiments were only performed to a 200-L waste drum limited by the experimental facility as shown in Fig. 5 (a). The diameter and height of 200-L drum are 56 and 90 cm, respectively. The waste drum was filled with polyamide with a density of 1.15 g/cc. Two small size sources

TABLE II

COMPARISON OF EXPERIMENTAL RESULTS BETWEEN SGS AND IM

Nuclide	r_{real} (cm)	C_{A} (1/s)	C_{B} (1/s)	SGS	IM	
				A/A_{real}	r	A/A_{real}
Cs-137	0	71	3	0.63	0	0.94
	8	78	23	0.69	7	0.95
	24	128	123	1.14	23	0.97
Co-60	0	77	5	0.85	0	0.91
	8	80	27	0.88	7	0.92
	24	94	99	1.03	23	0.94

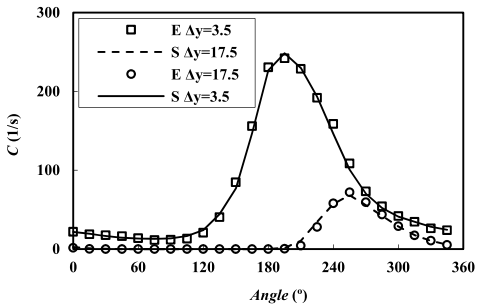

Fig. 6. Comparison of gamma count rates (C) between experiments labeled E and simulation labeled S when the detector is located at two deviated positions $\Delta y = 3.5$ and 17.5 cm. The abscissa is the angle position where the detector rotates around the waste drum.

with Cs-137 and Co-60 individually were set in the hole one by one within the matrix as shown in Fig. 5(b). The waste drum was rotated continuously. A Canberra's coaxial HPGe detector was employed in the experiments. The relative efficiency of the detector is 40%. The diameter and length of the sensitive crystal are about 6.2 and 5.95 cm, respectively. The detector was housed by a cylinder lead collimator with a square hole of 10×25 cm^2.

The count rates of full energy peaks in experiments are shown in Table II. The final results by SGS and the improved method (IM) are also listed in the table. The polar radii of the nuclide positions are 0, 8, and 24 cm. The detection efficiency was calibrated by experiments. It is found in the table that the equivalent radius obtained by IM is very close to the real radius (r_{real}). Accordingly, the ratio of the measured activity to the real activity is larger than 0.9, which means the relative error of less than 10%. At the same time, the minimum ratio (A/A_{real}) of SGS is 0.63 for Cs-137, 0.85 for Co-60. IM exhibits a better accuracy than that of SGS for 200-L waste drum.

In order to statistically analyze the assay performance for 400-L drum, a large number of numerical experiments were performed using the method studied by Qian *et al.* [10] and validated by MCNP in Forschungszentrum Julich. The method was also validated by the experiments as shown in Fig. 6. The Cs-137 source was set in the hole as shown in Fig. 5(b), whose radial distance to the drum axis was 9 cm. The detector was placed at two deviated positions with the offsets (y) of 3.5 and 17.5 cm. The waste drum was rotated and stopped with the angular spacing of 15° for measurement until the whole segment has been scanned. It can be seen in Fig. 6 that the count rates obtained by experiments agree well with simulation results. The maximum relative errors

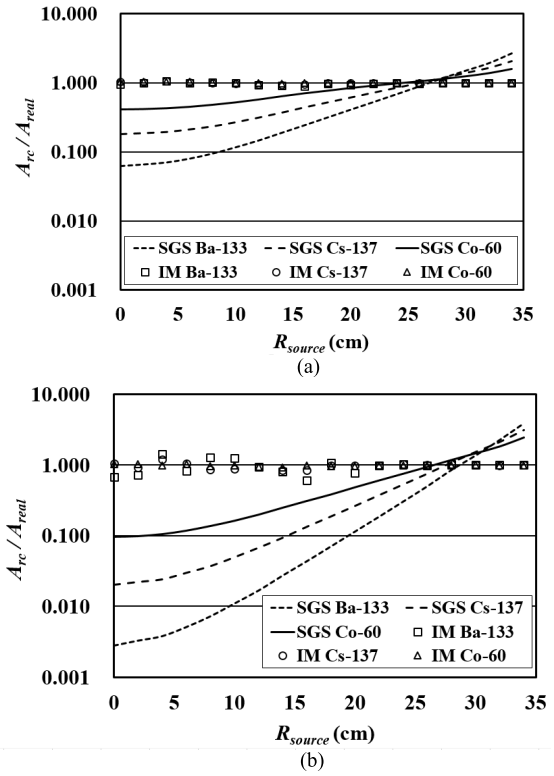

Fig. 7. Measured results for a line source that is positioned in the waste drum parallel to the drum axis. (a) The matrix density is 1.5 g/cc. (b) The matrix density is 2.5 g/cc.

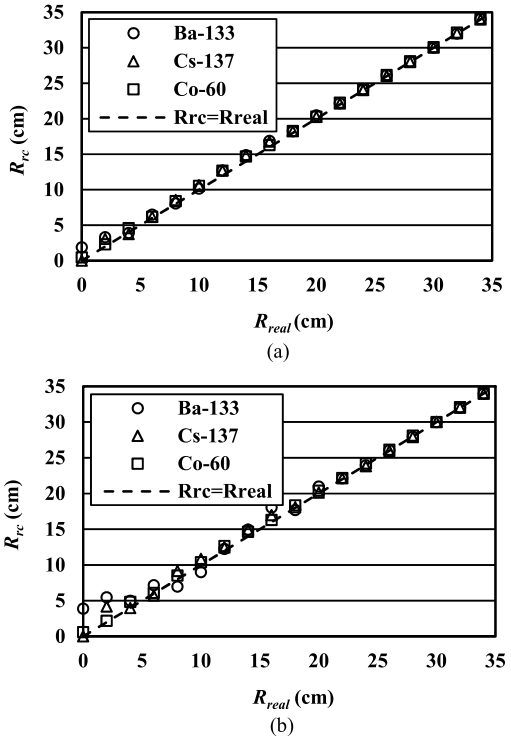

Fig. 8. Identified radius of a line source that is positioned in the waste drum parallel to the drum axis. (a) The matrix density is 1.5 g/cc. (b) The matrix density is 2.5 g/cc.

are 3% and 5%, respectively, when the detector is located at $y = 3.5$ and 17.5 cm. The relative error is close to the source uncertainty (5%), which proves the accuracy of the simulation.

As to the 400-L standard drum, the diameter and height are 70 and 105 cm. The main dimensions of the detection system adopted in the simulation were shown in Fig. 1. The offset between positions A and B was 24.5 cm. The waste drum was divided into seven segments. The height of one segment was 15 cm. Two types of the matrix with the densities of 1.5 and 2.5 g/cc were filled in the waste drum. Three nuclides, Ba-133 (0.356 MeV), Cs-137 (0.662 MeV), and Co-60 (1.333 MeV) were selected. The mass attenuation coefficients to gamma rays through the concrete were 0.11, 0.075, and 0.054 cm^2/g for these three nuclides [11].

In order to validate whether the equivalent radius was equal to the real radius, a line source with length 105 cm was set in the waste drum parallel to the drum axis. The final results are shown in Fig. 7, where $A_{\rm rc}$ is the measured activity, $A_{\rm real}$ is the real activity, and $R_{\rm source}$ is the radial distance of the line source to the drum axis. If $A_{\rm rc}/A_{\rm real}$ is equal to 1, which means the measured activity equal to the real activity. The figure shows that $A_{\rm rc}/A_{\rm real}$ in SGS markedly deviates from 1 when the source was located in the two regions near the drum center and drum wall. When the density of matrix increases from 1.5 to 2.5 g/cc, the minimum value of $A_{\rm rc}/A_{\rm real}$ for Co-60 is less than 0.1, which means that the measured activity is only 10% of the real activity. The error is similarly large for Ba-133 and Cs-137. At the same time, $A_{\rm rc}/A_{\rm real}$ in IM is very close to 1 wherever the source was located. The maximum values of $A_{\rm rc}/A_{\rm real}$ are 1.65, 1.21, and 1.08 for Ba-133, Cs-137, and Co-60, respectively, when the matrix density is 2.5 g/cc.

Fig. 8 shows the equivalent radius obtained by IM. Since only one line source existed in the waste drum, the measured equivalent radius should be equal to the real radius. The figure shows good agreement between the measured radius and the real radius. It proves that IM can determine the source position accurately. In Fig. 8(b), somewhat differences appear in the areas at $R_{\rm real} < 10$ cm when the matrix density is 2.5 g/cc. It is due to the flat distribution of detection efficiency ratio shown in Fig. 3(b), which results in the difficulty in determining the source radius.

In addition, multiple sources had been adopted in numerical experiments where 100 waste drums were assayed for one case. The numbers of point sources were 7 and 14. They were spread randomly in the 400-L waste drum.

Because the measured activity $A_{\rm rc}$ will be several times larger or less than the real activity $A_{\rm real}$, the relative activity residuals $(A_{\rm rc}-A_{\rm real})/A_{\rm real}$ can be several hundred percentages if $A_{\rm rc}$ is larger than $A_{\rm real}$, but only ranges from -100% to 0 if $A_{\rm rc}$ is less than $A_{\rm real}$. In order to reduce the influence of extreme errors on the statistical results, the geometric mean assay errors are adopted instead of arithmetic mean errors

$$\text{Mean} = \left(\prod_{n=1}^{N} \Delta_n\right)^{\frac{1}{N}} \tag{11}$$

To avoid Δ canceling each other when it is larger or less than 1, the relative activity (Δ) is defined as

$$\Delta = \text{Max}(A_{\rm rc}, A_{\rm real})/\text{Min}(A_{\rm rc}, A_{\rm real}) \tag{12}$$

TABLE III

MAXIMUM AND MEAN ASSAY ERRORS FOR SEVEN RANDOMLY DISTRIBUTED RADIOACTIVE SOURCES IN THE WASTE DRUM

Nuclide	Δ	Density=1.5g/cc		Density=2.5g/cc	
		SGS	IM	SGS	IM
Ba-133	Max.	2.96	2.01	8.06	3.11
0.356 MeV	Mean	1.34	1.19	1.66	1.43
Cs-137	Max.	2.03	1.58	4.13	2.53
0.662 MeV	Mean	1.23	1.10	1.46	1.29
Co-60	Max.	1.51	1.40	2.56	1.91
1.333 MeV	Mean	1.14	1.05	1.30	1.15

TABLE IV

MAXIMUM AND MEAN ASSAY ERRORS FOR 14 RANDOMLY DISTRIBUTED RADIOACTIVE SOURCES IN THE WASTE DRUM

Nuclide	Δ	Density=1.5g/cc		Density=2.5g/cc	
		SGS	IM	SGS	IM
Ba-133	Max.	2.05	1.67	3.29	2.64
0.356 MeV	Mean	1.21	1.16	1.39	1.32
Cs-137	Max.	1.64	1.30	2.48	1.87
0.662 MeV	Mean	1.14	1.08	1.28	1.21
Co-60	Max.	1.32	1.15	1.89	1.45
1.333 MeV	Mean	1.08	1.04	1.19	1.12

where Max and Min are the functions to determine the larger and smaller value between A_{rc} and A_{real}. In this case, Δ represents the times between the two activities and is never smaller than 1.

Tables III and IV show the maximum and geometric mean values of Δ when 7 and 14 randomly distributed sources were set simultaneously in one drum. The tables show that the detection accuracy is improved when the nuclide energy increases. When the matrix density is 2.5 g/cc in Table III, the maximum Δ of SGS for Ba-133, Cs-137, and Co-60 are 8.06, 4.13, and 2.56, respectively, which means that the measured activity will probably be about 8, 4, and 2.6 times larger or smaller than the real activity. However, both the maximum and mean Δ by IM are less than that of SGS. For example, when the density is 1.5 g/cc, the mean Δ of Co-60 by SGS and IM are 1.14 and 1.05, respectively, which means that the relative errors of measured activity are 14% and 5%. The similar results appear for nuclides of Ba-133 and Cs-137. In total, the relative errors of IM are reduced by half compared with the SGS. When the density becomes 2.5 g/cc, the strong attenuation of gamma rays due to the high density will lead to the decrease in gamma rays counts and the relative errors for both SGS and IM are nearly doubled. The mean relative errors of SGS are 66% for Ba-133, 46% for Cs-137, and 30% for Co-60, whereas the mean errors of IM are 43%, 29%, and 15% for the three nuclides. These values are reduced by about one third or a half.

When the source number increases from 7 to 14, the distribution of sources will become increasingly uniform, so the assay errors of SGS are reduced. As shown in Table IV, the mean relative errors of SGS are 21%, 14%, and 8% for Ba-133, Cs-137, and Co-60, respectively, when the density is 1.5 g/cc, and 39%, 28%, and 19% when the density is 2.5 g/cc. If IM is applied, the mean relative errors are 16%, 8%, and 4% when the density is 1.5 g/cc, and 32%, 21%, and 12% when the density is 2.5 g/cc, which decreases by 5% to 7% relative to SGS. It can be inferred that when more randomly distributed sources coexist in the waste drum, the assay errors of SGS will be further reduced. As to the IM, the increase of sources number will request the adjustment of the bias of equivalent radius *r*. The present results prove that it is optimum to apply the mean value of *r* in determining the equivalent radius. If the nuclides are more uniformly distributed, *r* should become larger and even take the maximum value. Therefore, the preanalysis on wastes is necessary before scanning.

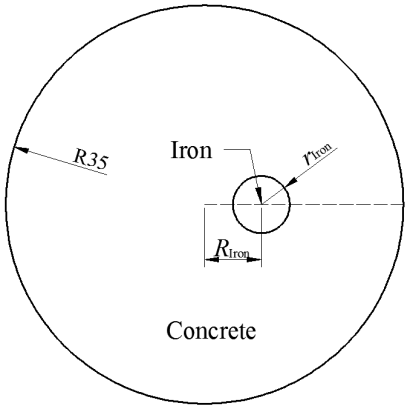

Fig. 9. Segmental sketch of a waste drum in which a cylindrical iron product is solidified in the concrete.

The IM is based on the assumption that the matrix in the waste drum is uniformly distributed. If it is not in the practical situation, IM will also assume the matrix is uniform. The mean density is obtained by the transmission measurement or weighing the whole waste drum. The nonuniformity of the matrix will affect the assay accuracy for both SGS and IM unless the matrix distributed image is reconstructed by TGS. In order to analyze the influence of matrix nonuniformity on assay accuracy of IM, a simple concrete solidified waste drum was adopted where a cylindrical iron was nested inside the concrete. Fig. 9 shows the section of a 400-L waste drum that contains a cylindrical iron product contaminated by radionuclides. Tow radii (r_{Iron}) of the cylinder, 5 and 10 cm, are selected. The radionuclides are assumed to be distributed uniformly on its surface. The cylinder is set individually in three positions whose polar radius (R_{Iron}) is 0, 15, or 25 cm, respectively. The numerical assay has been performed aiming at this section, and the results are shown in Tables V and VI.

The tables show that the assay errors in these cases are larger than those when one point source is inside the waste drum. Due to the strong attenuation of gamma rays by the iron, the detector can receive a part of gamma rays mainly from the radionuclides distributed on parts of the surface facing the detector. As a result, the identified radius (r) is a little smaller than the polar radius of the point on the cylinder surface nearest to the detector. When the cylinder is set in the drum center, the assay error is large for IM although the identified radius (r) is quite close to the cylinder radius, especially for Ba-133 emitting low-energy gamma rays and when the cylinder radius is 10 cm. It is because the gamma rays are attenuated by the long distance of concrete, but the

TABLE V

ASSAY RESULTS FOR A 400-L WASTE DRUM IN WHICH A CYLINDRICAL IRON WITH A RADIUS OF 5 cm IS SOLIDIFIED IN THE CONCRETE

Nuclide	r_{Iron} (cm)	C_A/C_B	r (cm)	A_{SGS}/A_{real}	A_{IM}/A_{real}
Ba-133	0	0.91	4.6	0.0013	1.3491
	15	0.79	17.0	0.0220	1.0706
	25	0.64	27.4	0.3950	0.8487
Cs-137	0	0.91	4.6	0.0070	1.1468
	15	0.76	17.0	0.0531	1.0042
	25	0.63	27.4	0.5066	0.8589
Co-60	0	0.90	4.9	0.0337	1.0020
	15	0.74	16.3	0.1242	0.9469
	25	0.61	26.3	0.6305	0.8944

TABLE VI

ASSAY RESULTS FOR A 400-L WASTE DRUM IN WHICH A CYLINDRICAL IRON WITH A RADIUS OF 10 cm IS SOLIDIFIED IN THE CONCRETE

Nuclide	r_{Iron} (cm)	C_A/C_B	r (cm)	A_{SGS}/A_{real}	A_{IM}/A_{real}
Ba-133	0	0.88	9.1	0.0046	4.1065
	15	0.72	23.0	0.0828	0.9892
	25	0.58	31.7	1.8719	0.9845
Cs-137	0	0.87	8.8	0.0181	3.0775
	15	0.70	22.9	0.1476	0.8827
	25	0.59	30.1	1.6738	1.3377
Co-60	0	0.85	9.5	0.0653	1.9125
	15	0.69	22.5	0.2551	0.8486
	25	0.59	28.5	1.4504	1.4328

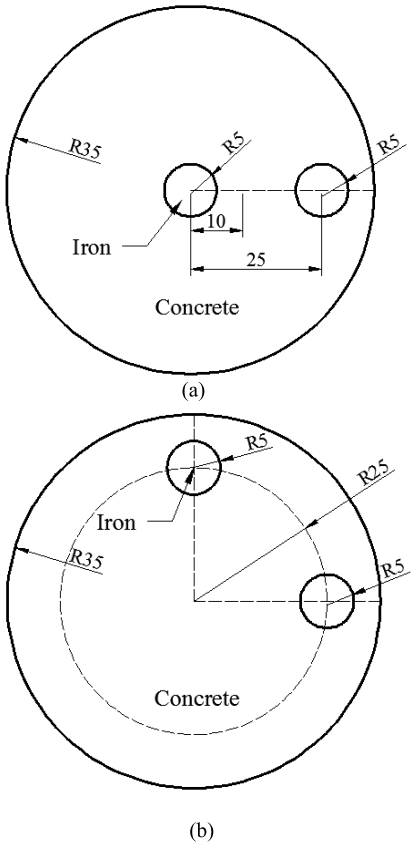

Fig. 10. Segmental sketch of a waste drum in which two cylindrical iron products are solidified in the concrete. (a) The sample of case 1. (b) The sample of case 2.

activity is calculated based on the matrix with the mean density larger than that of concrete. The whole sources distributed on the cylinder surface can also be equivalent to one point source, the equivalent radius depends on the size, density, and position of the cylindrical product. When the cylindrical iron is set far from the drum center, the shortest distance to the detector through the concrete will be shortened and the influence of attenuation by the iron will be enhanced so that the equivalent radius will be close to the polar radius of the cylinder (R_{Iron}) and depends on the gamma-ray energy. For example, the equivalent radii for Ba-133 on the cylinder with a radius of 10 cm are 23 and 31.6 cm, respectively, when R_{Iron} are 15 and 25 cm. The equivalent radius is almost equal to the identified radius, so the assay error of IM is the smallest. For Cs-137 and Co-60, the gamma rays have a strong penetrating ability, so the equivalent radius will be smaller, and accordingly, the identified radius is also smaller than that of Ba-133. However, the equivalent radius is based on both iron and concrete and the identified radius is calculated by the mean density. When the cylinder has a large radius and is positioned near the drum wall, the iron is in charge of the attenuation to gamma rays from the backside of the cylinder surface against the detector, the equivalent radius will be a little larger than the identified radius. This causes $A_{\text{im}}/A_{\text{real}}$ larger than 1 for both Cs-17 and Co-60 when the cylindrical iron is positioned at $R_{\text{Iron}} = 25$. As to SGS, the assay error is much larger than that of IM especially when the cylindrical iron is positioned in the drum center. Similarly, with the case of the point source, the nonuniformity of radionuclides is the main reason resulting in the low assay accuracy of SGS when radionuclides are concentrated on a product which is solidified in the concrete.

If more iron products are solidified in the waste drum, the assay accuracy is difficult to be predicted due to the unknown distribution of these products. Two samples, as shown in Fig. 10, are selected for the comparison. The sample of case 1 contains two cylindrical iron products with a radius of 5 cm which are positioned at $R_{\text{Iron}} = 0$ and 25 cm, respectively. The sample of case 2 also contains two cylindrical iron products with a radius of 5 cm which are positioned at $R_{\text{Iron}} = 25$ cm, but with a polar angle spacing of 90°. The same amount of radionuclides is distributed on the of both cylinders. The results are shown in Table VII. It can be found that the gamma count rates by detector B relative to detector A are similar to each other for both case 1 and case 2. The identified radii are also similar. It indicates that the radionuclides concentrated in drum center have few contributions to the detection. Therefore, the assay activity of case 1 is smaller than that when one cylindrical iron is positioned at $R_{\text{Iron}} = 25$ in Table V for both SGS and IM. At the same time, the assay activity of case 2 is similar with that in Table V. It can be seen that the identified radius in IM will be decided by the activity distribution of gamma rays and the strong attenuation by irons and concretes. The iron products with a large number of radionuclides positioned near the drum wall will easily affect the final assay results. Therefore, it is difficult to assay accurately the activity of

TABLE VII

ASSAY RESULTS FOR A 400-L WASTE DRUM IN WHICH TWO CYLINDRICAL IRON PRODUCTS WITH A RADIUS OF 5 cm ARE SOLIDIFIED IN THE CONCRETE

Case No.	Nuclide (cm)	C_A/C_B	r (cm)	A_{SGS}/A_{real}	A_{IM}/A_{real}
1	Ba-133	0.6423	27.5	0.2054	0.4549
	Cs-137	0.6306	26.9	0.2659	0.4854
	Co-60	0.6240	25.3	0.3428	0.6075
2	Ba-133	0.6414	27.6	0.4095	0.8771
	Cs-137	0.6270	27.2	0.5249	0.8854
	Co-60	0.6103	26.5	0.6524	0.9199

the radionuclides deep in the waste drum. This is a common problem for SGS, IM, and even TGS.

IV. CONCLUSION

An improved characterization assay algorithm is developed for 400-L low- and intermediate-level radioactive waste drum based on the assumption of the segmented equivalent ring source. IM proposes that the nuclides in the waste drum are treated as ring sources and accumulated in one segment. The equivalent radius of the ring source is estimated by applying two detectors at different positions. The assay accuracy can be improved because the detection efficiency is calibrated accurately based on the equivalent ring source.

This method was validated by experiments on a 200-L waste drum which was filled with polyamide. The Cs-137 and Co-60 point sources were set in the waste drum at three different positions. The experimental results show that the assay errors by IM are greatly less than that of SGS.

The assay process for 400-L waste drum was performed by numerical simulations. Three nuclides, Ba-133, Cs-137, and Co-60, and two matrix densities,1.5 and 2.5 g/cc, were selected. The results show that IM can determine accurately the source positions by using two detectors and has better accuracy than SGS if the matrix is uniformly distributed in the waste drum. The detection accuracy depends on the matrix density, nuclide type, and number sources. The maximum errors of IM are several times smaller than that of SGS. The mean errors are reduced almost by one third to a half for all nuclides.

The IM is also applied in assaying the solidified wastes drum. The cylindrical iron products are assumed to be solidified in the concrete. The radionuclides are distributed on the cylinder surface. The strong attenuation of gamma rays by irons and concretes will affect the determination of source positions and lead to a decrease in assay accuracy. However, it is overall better than that of SGS if one or two iron products are solidified inside the waste drum.

This study demonstrates that IM is an accurate method in assaying the compacted waste drums filled with high-density matrix when radioactive sources are distributed nonuniformly.

REFERENCES

[1] E. R. Martin, D. F. Jones, and J. L. Parker, "Gamma-ray measurements with the segmented gamma scanner," Los Alamos Scientic Lab., Santa Fe, NM, USA, Tech. Rep. LA-7059-M, 1977.

[2] F. Bronson, V. Atrashkevich, G. Geurkov, and B. Young, "Probabilistic uncertainty estimator for gamma-spectroscopy measurements," *J. Radioanal. Nucl. Chem.*, vol. 276, no. 3, pp. 589–594, Jun. 2008.

[3] R. J. Estep, T. H. Prettyman, and G. A. Sheppard, "Tomographic gamma scanning to assay heterogeneous radioactive waste," *Nucl. Sci. Eng.*, vol. 118, no. 3, pp. 145–152, 1994.

[4] C. Liu, W. G. Gu, N. Qian, and D. Z. Wang, "Study of image reconstruction using dynamic grids in tomographic gamma scanning," *Nucl. Sci. Techn.*, vol. 23, no. 5, pp. 277–283, 2012.

[5] W. Gu, C. Liu, N. Qian, and D. Wang, "Study on detection simplification of tomographic gamma scanning using dynamic grids applied in the emission reconstruction," *Annu. Nucl. Energy*, vol. 58, pp. 113–123, Aug. 2013.

[6] W. Gu, K. Rao, D. Wang, and J. Xiong, "Semi-tomographic gamma scanning technique for non-destructive assay of radioactive waste drums," *IEEE Trans. Nucl. Sci.*, vol. 63, no. 6, pp. 2793–2800, Dec. 2016.

[7] Y. F. Bai, E. Mauerhofer, D. Z. Wang, and R. Odoj, "An improved method for the non-destructive characterization of radioactive waste by gamma scanning," *Appl. Radiat. Isot.*, vol. 67, no. 10, pp. 1897–1903, Oct. 2009.

[8] C. Liu, D. Z. Wang, Y. F. Bai, and N. Qian, "An improved segmented gamma scanning for radioactive waste drums," *Nucl. Sci. Techn.*, vol. 21, no. 4, pp. 204–208, Aug. 2010.

[9] T. T. Thanh *et al.*, "A prototype of radioactive waste drum monitor by non-destructive assays using gamma spectrometry," *Appl. Radiat. Nuclides*, vol. 109, pp. 544–546, Mar. 2016.

[10] N. Qian, T. Krings, E. Mauerhofer, D. Z. Wang, and Y. F. Bai, "Analytical calculation of the collimated detector response for the characterization of nuclear waste drums by segmented gamma scanning," *J. Radioanal. Nucl. Chem.*, vol. 292, no. 3, pp. 1325–1328, Jun. 2012.

[11] J. H. Hubbell, S. M. Seltxzer, *X-Ray Mass Attenuation Coefficients*, Standard 126, NIST, Jul. 2004.